








Artificial Intelligence based Multi-Objective Hybrid Controller for PV-Battery Unified Power Quality Conditioner

Koganti Srilakshmi* , Sravanthy Gaddameedhi* , Sumanth Yamparala ** 
Srinivas Nakka *** , YSR Kamal* , B. Surendra Babu * , Guduguntla Anil * 

*Department of Electrical Engineering, Sreenidhi Institute of Science and Technology, Hyderabad, Telangana, 501301.

** Department of Electrical and Electronics Engineering, R.V.R & J.C. college of Engineering, Guntur, Aandhra Pradesh, 522019.

*** Department of Electrical Engineering, Vardhaman College of Engineering, Hyderabad, Telangana, 501218.

(kogantisrilakshmi29@gmail.com, sravanthi314@gmail.com, sumanth46@gmail.com, nakkasrinu@gmail.com, kamal2001@gmail.com,
bheemanathinisurendrababu@gmail.com, guduguntlaanil@gmail.com)

‡

Corresponding Author: Koganti Srilakshmi, Sreenidhi Institute of Science and Technology, Tel: +91-8885851666,
kogantisrilakshmi29@gmail.com.

Received: 11.02.2022 Accepted: 17.03.2022

Abstract: Integration of renewable energy sources into the distribution network and the usage of power electronics devices leads to the power quality (PQ) issues. FACTS devices are playing a vital role in eliminating PQ issues effectively. UPQC is one among the Multi-functional FACTS devices. This work presents an artificial intelligence-based hybrid control technique for the unified power quality conditioner (UPQC) integrated with solar PV and battery storage systems. The UPQC comprises a series and a shunt voltage source converter, connected with a dc link. UPQC eliminates the voltage and current based distortions simultaneously. The hybrid controller adapts both the Fuzzy Logic controller (FL-C) and artificial neural network (ANN). The Neuro-Fuzzy Hybrid Controller (NFHC) is adapted to control DC-Link voltage. The prime objectives of the proposed work are minimization of harmonics in current waveforms and power factor improvement, rapid action for dc-link voltage balancing, elimination of sag/swell in the source voltage, better performance for large disturbances, and suitable compensation for unbalanced networks. The performance analysis of the proposed controller was carried out with three different test cases for various combinations of loads, solar irradiation and compared with those of existing methods like proportional integral controller (PI-C), sliding mode controller (SM-C), and FL-C. The proposed method shows a superior performance in minimizing THD to 3.6%, 4.16%, and 2.5% for all the three test cases which is much lower than other methods.

Keywords- Power quality, UPQC, FL-C, PI-C, PWM, solar power generation, battery storage system, ANN

1. Introduction

The deterioration of PQ referring to the quality of voltage and current such as voltage sags/-swells, harmonics, interruptions, flickers, etc., is primarily due to the ever-growing usage of electric gadgets and nonlinear loads. The total harmonic distortion (THD) is an important measure of PQ and must be kept as minimum as possible. Lower THD helps in improving the efficiency, power factor, and overall life of equipment [1]. A novel synchronous-reference frame (SRF)-based controller was developed to UPQC for 3 ω -4wire distribution network in order to mitigate PQ issues [2]. Moreover, the development of intricate algorithms enables online control of active power filters and UPQCs

through different controllers such as PI-C, FL-C, and ANN [3-6] for enhancing their dynamic performances with dynamically varying nonlinear loads.

The solar PV integrated UPQC was developed and its performance was investigated with the goal of minimizing the THD, voltage distortions by extracting maximum power [7]. Various Intelligent Control structures employing fuzzy logic and neural networks for improving power quality in the distribution system was outlined [8]. A fuzzy control was employed for enhancing the performances of the UPQC in improving the PQ of the power system [9]. FLC based UPQC was presented to minimize the power quality issues and comparative analysis was carried out for both with and without UPQC [10]. The Predictive phase dispersion

modulation technique was developed for the Cascaded H-Bridge Multi-Level Inverter based UPQC with the objective of compensating the voltage sag/swell, current harmonics, and maintains constant DC-Link voltage [11].

The adaptive distributed power control method was developed for the two H-connected setup with eight switches of 3- ϕ UPQC with the aim of eliminating THD, voltage distortions [12]. PV/Wind/PEMFC fed multi-level cascade UPQC was developed with SVPWM technique in the view of minimizing supply voltage distortions and THD to 3.98% which is lower than SPWM [13]. THD mitigation with UPQC at steel plant for induction-furnace load was investigated and to shows its superiority the comparative analysis was carried out with synchronous compensator. The proposed method reduces THD from 54.29% to 0.85% while DSTATCOM was able to reduce it to 4.98% [14]. ANFIS technique based solar integrated UPQC was designed for power quality improvement and performance analysis was carried out for different load and supply conditions [15]. The hybridization of both the series and shunt-active power filters (SAPF & SHAPF) was suggested for building UPQC with a goal of providing compensation to voltage sags/swells, VAR, and harmonic currents. The method adapted a control scheme involving instantaneous power theory [16]. The functionality of UPQC was modified to give equal sharing to both SAPF and SHAPF, thereby reducing the rating of SHAPF and the overall cost of UPQC [17]. An artificial neural network (ANN) based controller was outlined for performing CC for SHAPF of UPQC, wherein the ANN was developed off-line using the data of classical proportional-integral controller (PIC) [18]. An exhaustive review was performed for presenting different UPQC configurations and various compensation schemes [19]. A scheme containing UPQC was suggested for a micro-grid comprising PV/Wind/Fuel cell/Battery systems with a view of addressing PQ related problem [20]. The performances of various PWM strategies and different space vector PWM techniques were discussed [21]. The benefits and challenges of integrating the renewable energy sources into the grid and their control strategies was studied [22]. The effects on the smart grid technologies on the national grid were highlighted and few suggestions were also given to convert conventional grid into smart grid [23]. The comparison between P & O and PSO algorithms to get MPP for the PV system was studied for solar irradiation changes [24]. Experimental set-up of isolated boost full bridge DC-DC converter was investigated along with a set of low loss active snubber circuit [25]. Integration of renewable sources to micro grid for MPPT was studies with power management [26]. High voltage isolated ACDC converters were developed based on the modular technology [27]. FDNE based method was developed based on online least square identification algorithm along with digital simulators [28]. Fuzzy logic controller was suggested for PV-MPPT to improve the overall performance by maximum power point tracking [29].

Though several methods were suggested in literature, there is still a scope for developing new techniques and controllers for effectively mitigating the PQ issues.

In this article, a hybrid controller involving fuzzy logic and ANN control for UPQC with solar PV (SPV) and

Battery storage (BS) has been proposed with a view of lowering the THD and improving the power factor under unbalanced source voltage with sag/swell and harmonic loading conditions. The performances of the proposed Neuro-fuzzy hybrid controller (NFHC) of UPQC with SPV and BS (U-PVB) for a test distribution system with three different test cases have been studied and compared with existing and conventional PI controllers.

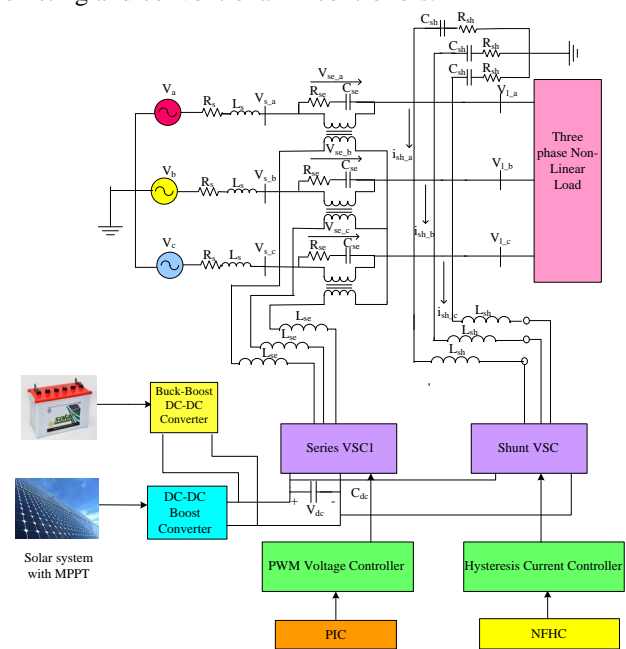


Fig. 1. Structure of UPQC with SP and BS (U-PVB)

2. Proposed U-PVB

Fig.1 illustrates the structure of UPQC supported with a Battery system (BS) and solar power (SP). The SP and BS are coupled to the DC-link of UPQC via a boost converter. This work proposes NFHC for exploiting both the properties of FL-C and ANN. V_a, V_b, V_c are the grid voltages, $V_{s,a}, V_{s,b}, V_{s,c}$ are bus voltages at the source side, R_s, L_s are source resistance, and inductance. UPQC comprises both series converter (SC) and shunt converter (SHC). The SC is a 3 ϕ - PWM voltage source converter (VSC), which mitigates voltage sags/ swells, distortions, and supply voltage unbalances. Subsequently, the series RLC filter comprising of resistor R_{se} , inductor L_{se} and capacitor C_{se} is connected to prevent the flow of switching ripples.

Similarly, the transformers are connected to provide isolation between SC and the power line. It injects compensating voltage into the grid. The SHC consists of a 3 ϕ - hysteresis current control, which is connected through a resistance R_{sh} , interfacing inductor L_{sh} , capacitance C_{sh} to provide isolation between the SHC and power line. The purpose of SHC is to restrain the current harmonics and control the DC-link capacitor voltage (V_{dc}) with low

settling-time without overshoot by injecting suitable current i_{sh} . The balanced 3ω rectifier load, 3ω unbalanced R-L load, and induction furnace load has been taken in the proposed work. The proposed UPQC specifications, ratings of loads considered are exhibited in Table- 4.

Table1. BS and SPV ratings

Device	Parameters	Values
Li-ion battery	Rated battery capacity	350 Ah
	Maximum battery capacity	450 Ah
	Nominal-voltage	650 V
	Fully-charge voltage	756 V
Solar-PV panel (SPR-215-WHT-U)	Rated Power	214.92 W
	Open circuit voltage	48.3 V
	Short circuit current	5.8 A
	Voltage/current at maximum power	39.8 V /5.4A
	Number of parallel cells	11
	Number of series cells	18

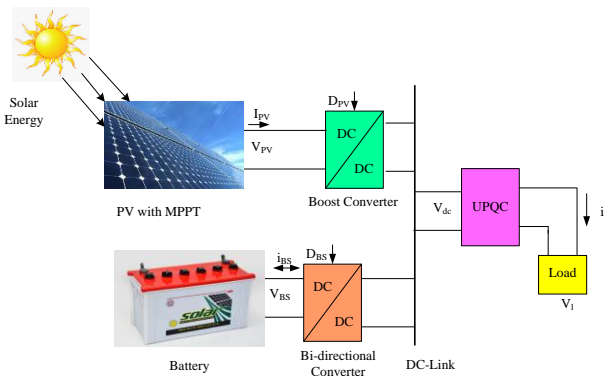


Fig. 2. Schematic Diagram of external support of DC-Link

2.1 External support for DC-Link

The SPV and the BS support the DC-bus through a DC-DC boost converter and BBC respectively for improving the stability of the UPQC in compensating PQ problems as shown in Fig. 2. The power balance equation of this arrangement is given by Eq. (1).

$$P_{PV} + P_{BS} - P_{dclink} = 0 \quad (1)$$

Where,

P_{PV} and P_{BS} denote the power supplied by Solar and Battery respectively

P_{dclink} represents the load at DC-link.

2.1.1 Solar Power System (SP)

The solar power system is used to convert solar energy into electrical energy. The SPV controller consists of a solar-PV panel, boost converter (BC) with MPPT shown in Fig.3. The production of electricity depends on solar irradiation incidents on PV cells.

The MPPT is applied to extract maximum output voltage from the PV cell under the precise irradiance/ temperature. The basic model of the PV cell is as shown in Fig. 4. The output power P_{PV} of the PV panel can be calculated by Eq. (2)

$$P_{PV} = V_{PV} \cdot I_{PV} \quad (2)$$

Where, V_{PV} , and I_{PV} are the solar PV panel output Voltage and Current. In this work, MPPT adopts the well known Perturb and observes (P & O) method to control the duty cycle (D) of the boost converter. The ratings of SPV, BS are given in Table-1.

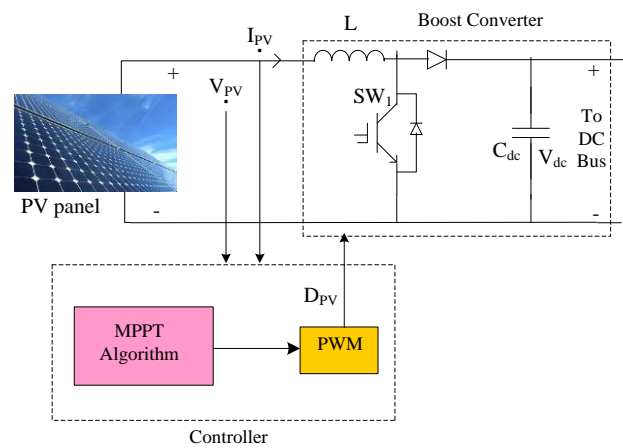


Fig. 3. Solar PV system with controller

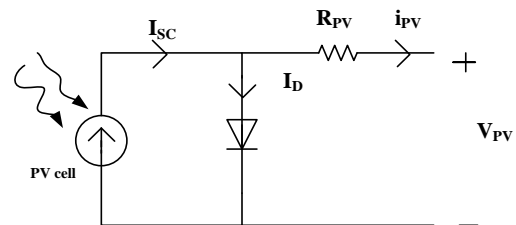


Fig. 4. Model of PV solar cell.

2.1.2 Battery storage (BS)

The BS consists of a battery and a bidirectional DC-DC buck-boost converter with PI-C, Which is responsible for maintaining the DC bus voltage as shown in Fig. 5. The state of charge (SOC) is given by Eq. (3).

$$SOC = 100(1 + \int i_{BS} dtQ) \quad (3)$$

The battery functions in two stages; charging and discharging, which depend on the power produced by solar. The working of the battery depends on energy constraints which are determined by the SOC limits given by Eq. (4).

$$SOC_{min} \leq SOC \leq SOC_{max} \quad (4)$$

Where,

Q is the battery capacity.

V_{BS} indicates the battery voltage.

i_{BS} indicates the battery current.

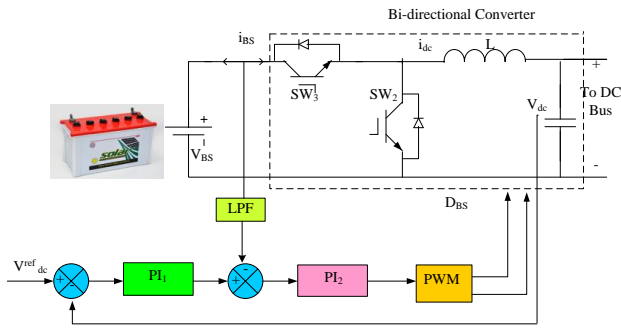


Fig. 5. Battery system with Bi-Directional Buck-Boost controller

PI_1, PI_2 controller gains are heuristically chosen as $K_{p1} = 1.5, K_{i1} = 0.1, K_{p2} = 1.477$ and $K_{i2} = 3.077$ respectively. Table 2 explains the power distribution under different operating conditions of the U-PVB.

Table 2. Power Distribution at DC-link

Level of solar power generation	Power Distribution
Solar power generated > DC-link power demand	BS charge still it attains maximum SOC
Solar power generated = DC-link power demand	SP alone supplies the DC-link's power demand.
Solar power generated < DC-link power demand	BS supplies the difference power till it reaches the lowest discharging limit
No solar generation	BS supplies DC-link's power demand.

2.2 Shunt Controller

The role of the shunt-VSC is to suppress the supply harmonic currents by injecting suitable compensating current at PCC and to maintain constant dc-link voltage. The hybrid controller for shunt-VSC adapts (i) abc-dq0 and dq0-abc domain conversions; (ii) NFHC is used for reducing current harmonics and maintaining dc-link voltage. The load current is converted into the dq0 domain employing the phase and frequency information of the grid voltage using PLL. NFHC compares dc-link voltage with a reference voltage and transforms the error voltage into a required change in current for maintaining the dc-link voltage. The d-th component load current is added with the error current signal derived from NFHC to produce referenced current. The dq0 components are again converted into abc domain, which is compared with the actual load currents in a hysteresis current controller to produce gating pulses for shunt VSC. The schematic of the NFHC is depicted in Fig. 6. As the transformation of currents from abc to dq0 and then to abc domain are available in the literature, the design of the NFHC control part is explained below:

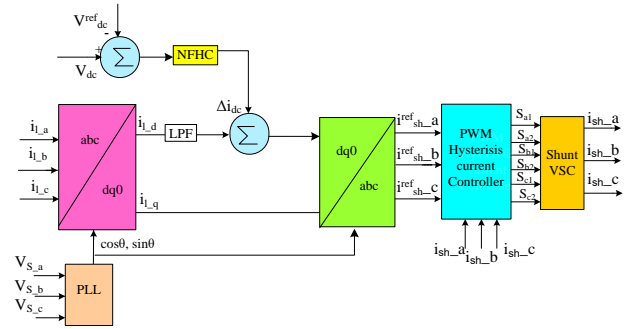


Fig. 6. NFHC for Shunt converter

2.2.1 Proposed NFHC

The NFHC is a combination of a fuzzy logic control mechanism whose process is inspired by the neural network technique. The fuzzy logic controller is based upon mathematical reasoning that works on designated linguistic rules. The fuzzy logic control consist set of fuzzy rules which export the output as linguistic variables instead of numerical values. The fuzzy logic controller operates on three mechanisms fuzzification, inference, and defuzzification. Fuzzification is the process of conversion of numerical values into linguistic variables. A set of membership functions are defined to evaluate the variables. A set of membership functions (MF) are defined to evaluate the variables. Based upon the membership functions the variables take a specific linguistic value. The membership functions and the set of rules are determined at the inference stage. Based on the input, the output takes any one of the values in the defuzzification stage. The overall fuzzy controller is shown in Fig.7.

The Takagi–Sugeno fuzzy model takes error (E) and rate of change of error (COE) as inputs. The error is calculated by Eq. (5). Triangular MF is used for an error and change in error of the FL-C as given in Figs.8 and 9 respectively. The linguistic variables for E, COE, D are given as ‘‘PSH’’ – Positive-High, ‘‘PSM’’ – Positive-Medium, ‘‘PSL’’- Positive-Low, ‘‘ZO’’ – Zero, ‘‘NEL’’ – Negative-Low, ‘‘NEM’’ – ‘‘Negative-Medium, and ‘‘NEH’’ – Negative-High. Fuzzy ‘‘IF-THEN’’ rules are developed using these linguistic variables. The value of the DC link voltage takes values in-between any of these linguistic variables. The DC link voltage is made to be operated within a set of membership functions hence a total of 49 possible sets are obtained which is given in Table 3.

$$E = V_{dc}^{ref} - V_{dc}^i; i = 1,2,3,4,5,6 \quad (5)$$

The neural network is an adaptive control technique that works identical to the human brain. The neural network controller can train itself based upon the different working conditions. The neural network consists of interconnected neurons which are trained to work based on requirement. The network consists of input, an output layer, and numerous hidden layers are embedded between the input and output layers. These hidden layers are allocated with specific weights and based upon the weights of the layer the priority is assigned at each stage.

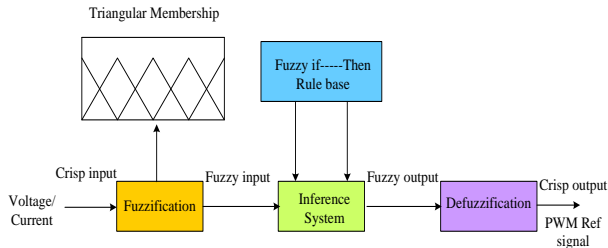


Fig. 7. Overview of Fuzzy controller

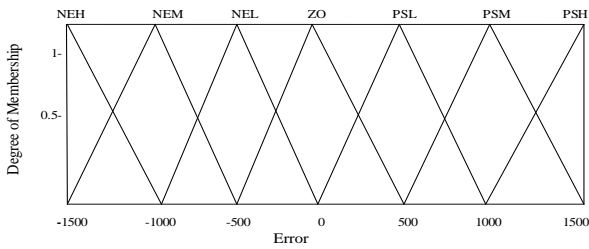


Figure 8: MF for error

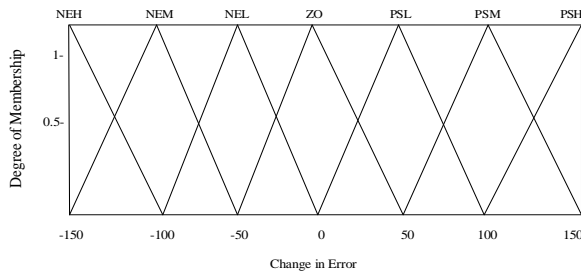


Fig. 9. MF for change in error

Table 3. MF mapping for DC-Link voltage

E	COE						
	PSH	PSM	PSL	ZE	NEL	NEM	NEH
NEH	ZE	NEL	NEM	NEB	NEH	NEH	NEH
NEM	PSL	ZE	NEL	NEM	NEH	NEH	NEH
NEL	PSM	PSL	ZE	NES	NEM	NEH	NEH
ZE	PSH	PSM	PSL	ZE	NEL	NM	NEH
PSL	PSH	PSH	PSM	PSL	ZE	NEL	NEM
PSM	PSH	PSH	PSH	PSM	PSL	ZE	NEL
PSH	PSH	PSH	PSH	PSH	PSM	PSL	ZE

The proposed adaptive neuro-fuzzy controller is a more reliable adaptive controller that combines the functionality of both the neural network and fuzzy logic mechanism. The inputs are first trained according to the membership functions and then the inputs are fed to the neural networks and based upon the number of hidden layers the controller gets trained and output is got after proper evaluation. The overview of the proposed NFHC is shown in Fig.10. The triangular inference output is trained by the hybrid neural network algorithm to generate the optimized output. In the

PV integrated UPQC system V_{dc}^{ref} is compared with reference V_{dc}^{ref} signal, the DC link voltage sensed from the DC link capacitor is fed to the NFHC controller. The ANN system is trained with the Levenberg-Marquardt algorithm.

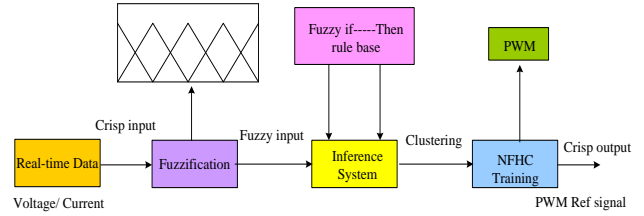


Fig. 10. Overview of NFHC

The NFHC system can be modeled mathematically as two input parameters (u and v) with an AND operator to get the output (z) can be expressed as Equation (6).

$$\text{IF } u \text{ is } X \text{ and } v \text{ is } Y, \text{ then } z = f(u, v) \quad (6)$$

There exist five layers, consider the membership function at the fuzzification layer with first input u is expressed as $\beta_{xj}(u)$, the membership functions used is denoted by j . The AND operator is implemented in the second layer, the neurons at the second layer are given in Equation (7).

$$w_i = \beta_{xj}(u) * \beta_{yj}(v) \quad (7)$$

The third layer contributes to the normalization of the values from the second node. The normalized values in the third layer are expressed in Equation (8).

$$w_i = \frac{w_i}{w_1 + w_2} \quad (8)$$

The self-adaptive property of the ANN controller is implemented by using the inference parameters (a_i, b_i, c_i) in the fourth node through Equation (9).

$$\overline{w_i f_i} = w_i (a_i u + b_i v + c_i) \quad (9)$$

The inputs get summed up at the fifth layer to generate the output given in Equation (10).

$$f = \sum_i \overline{w_i f_i} \quad (10)$$

The block diagram representing the five layers of the NFHC system with two input parameters is as shown in Figure 11. The fuzzy rules that apply to the structure are given as Eq. (11) - (12).

$$\text{If } u \text{ is } X_1 \text{ AND } v \text{ is } Y_1, \text{ then } f_1 = a_1 u + b_1 v + c_1 \quad (11)$$

$$\text{If } u \text{ is } X_2 \text{ AND } v \text{ is } Y_2, \text{ then } f_2 = a_2 u + b_2 v + c_2 \quad (12)$$

The NFHC system works based on the above mathematical equations.

2.3 Series Controller

The control signals are generated by comparing the load voltage with reference voltage after transformations from the abc-to-dq0 domain and then the reference voltage signals are generated with PI-C in the d-q domain and again converted to abc domain, as shown in Fig. 12. The control

signals serve as gating pulses for performing PWM in a series converter. The k_p , k_i values of PI-C are chosen arbitrary as 1.32, 0.01 respectively.

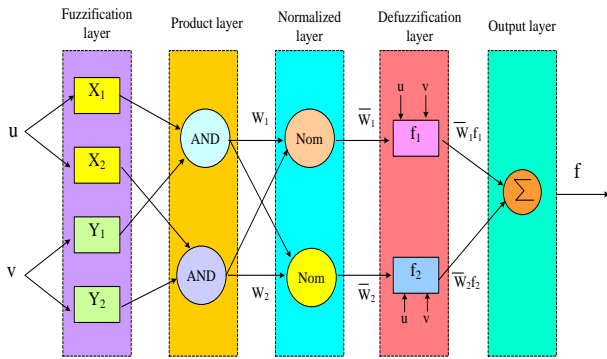


Fig. 11. Structure of NFHC

3 Results and Discussions

The proposed UPQC with SP and BS (U-PVB) was studied on a 3- ϕ AC distribution system. The Simulation model for the U-PVB has developed in Matlab 2016a is shown in Fig. 13. Three different test cases with various combinations of loads, conditions like sag/ swell and, variation in solar irradiation from 1000W/m² to 800W/m² as given in Table 5, were considered for studying the performances of the U-PVB.

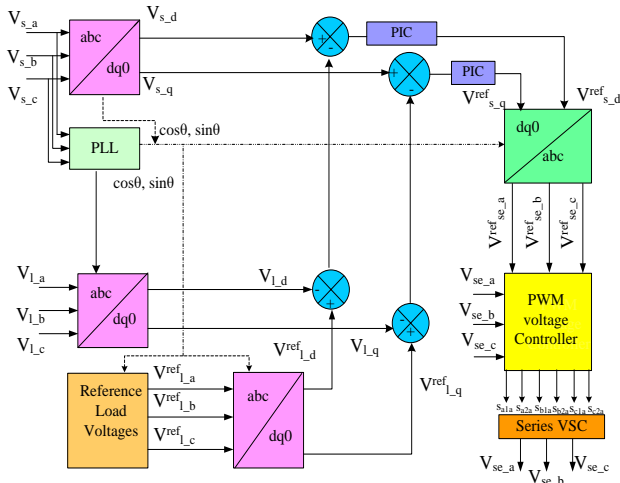


Fig. 12. Controller for Series Converter

The source voltage is considered balanced with voltage sag/ swell, disturbance for cases 1-2, and unbalanced for case 3. The solar irradiation variation is as shown from case1 to case2. The results are compared with existing methods available in the literature. The THD for source current (I_s) of the U-PVB was obtained for all the test cases and compared with those PI-C, SM-C, FL-C, and NFHC in Fig.14. The power factor (PF) at the source side of the proposed NFHC calculated by Eq. (16) for all test cases and comparison is as shown in Fig.15.

$$Powerfactor = \cos \theta * \frac{1}{\sqrt{1 + THD^2}} \quad (13)$$

Where, θ is the measured angle between voltage and current, while $\frac{1}{\sqrt{1 + THD^2}}$ represents displacement factor.

Table 4. UPQC specifications and loads

Source	Voltage: 415V , Frequency: 50Hz Resistance: 0.10 Ω , Inductance: 0.150mH
Series compensator	Resistance: 1.0 Ω , Inductance: 3.60 mH ; Capacitance: 60.0 μ f
Shunt compensator	Resistance: 0.001 Ω , Inductance: 2.15 mH, Capacitance: 1.0 μ f , VSC hysteresis controller band: 0.010A
Dc-Link	Capacitance: 9400.00 μ f ; Voltage: 700.0V
Loads	Balanced-3 ϕ Rectifier Load: 30.0 Ω & 20.0mH
	Unbalanced-3 ϕ RL Load R: 10.0, 20.0 &15.0 Ω ; L: 9.50, 10.50 & 18.50 mH.
	Induction Furnace load: LC = 400.0 mH,50.0 Mf, RL = 10.0 Ω ,100.00 mH

The source voltage (V_s), injected voltage (V_{inj}), load voltage (V_l), dc-link voltage (V_{dc}), load current (i_l), injected current (i_{inj}), source current (i_s) waveforms during steady state as well as sag/swell, disturbance conditions of the U-PVB for test cases 1-3 are shown in Fig. 16-18.

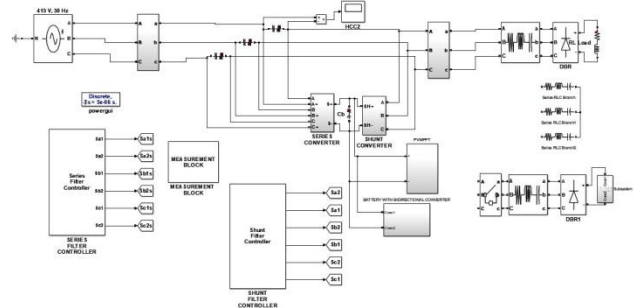


Fig. 13. Simulink model of UPVB along with test system

In case1, the voltage was sagged by 30% during the interval 0.2-0.3s and swelled by 30% during 0.4-0.5s. The voltage disturbance was introduced during 0.6-0.7 s, as shown in Fig. 16(a). Moreover, the load current was non-sinusoidal but balanced with a THD of 22.67% and a PF of 0.789 due to nonlinear rectifier load is presented in Fig. 16(b). It can be seen from Fig. 16 that the U-PVB can provide a more stable load voltage and sinusoidal source current. Such enhancement in current waveforms also reflected in the THD and PF values the THD of the load current was reduced from 22.67% to 3.60%, which is smaller than those of the existing methods [18], and the PF rose from 0.789 to 0.989 by injecting appropriate series

voltages and shunt currents. It is also seen from Fig. 16 (c) that under constant irradiation of 1000W/m² the NFHC was able to quickly settle the dc-link voltage to the steady-state around 0.04 s and maintain the voltage constant.

In case2, the voltage sag, swell, and disturbances introduced are similar to case1, shown in Fig. 17(a). Here, the load current was sinusoidal but unbalanced with a THD of 18.88% and a power factor of 0.623 due to nonlinear unbalanced load as presented in Fig. 17(b). It is seen that the U-PVB was able to eliminate sag/swell and disturbances effectively and reduce THD from 18.88% to 4.16% thereby improving PF value from 0.623 to 0.985 as given in Fig. 16-18 respectively by injecting suitable shunt currents. It is also seen from Fig. 17 (c) that when irradiation variation from 1000W/m² to 600 W/m² PV current reduces from 14.87A to 8.928A and voltage reduces from 19.98V to 9V the U-PVB was able to quickly settle the dc-link voltage to the steady-state voltage around 0.04 s and maintains the voltage constant.

In case3- the unbalanced supply voltage under constant irradiation of 1000W/m² was considered shown in Fig. 18(a). The load current was sinusoidal and unbalanced with a THD of 11.91% and a PF of 0.875 Fig. 18(b). The NFHC is able to reduce the THD from 11.91% to 2.50% and improve PF from 0.875 to 0.999 by injecting suitable shunt currents and maintaining the voltage is constant as shown in figure 18(c). It also settles the dc-link voltage to the steady-state voltage around 0.04s given in table 6. The THD spectrum for all test cases is as shown in Fig.19.

Table 5. Test cases considered

State of the system	Case1	Case2	Case3
Balanced source voltage	✓	✓	
Unbalanced source voltage			✓
Voltage Sag/ Swell, Disturbance	✓	✓	
Constant 1000 W/m ² irradiation	✓		✓
Irradiance from 1000 W/m ² to 800 W/m ²		✓	
Balanced-3 ϕ Rectifier Load	✓	✓	✓
Induction Furnace load			✓

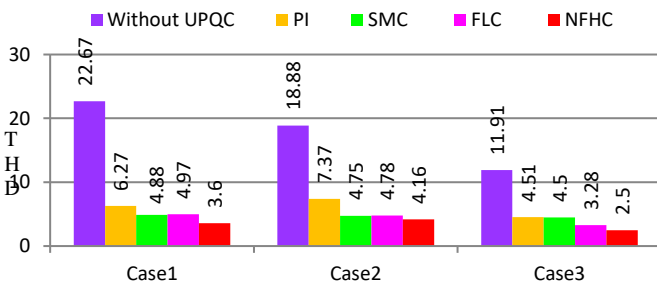


Fig. 14. THD comparison bar chat

Table 6. Settling-time of DC-Link voltage

Case	PI-C	SM-C	FL-C	NFHC
1	0.191	0.102	0.080	0.050
2	0.202	0.104	0.080	0.050
3	0.272	0.100	0.060	0.050

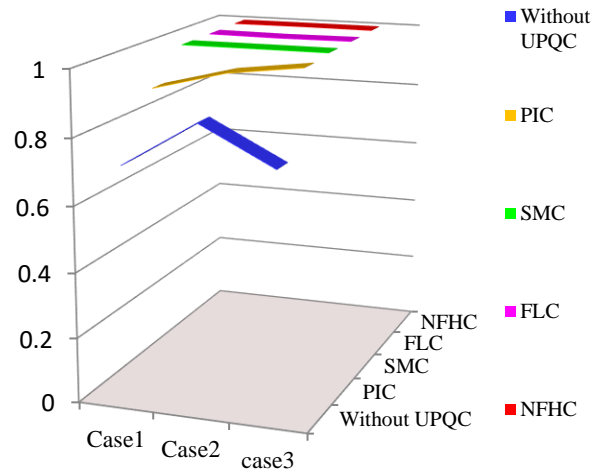
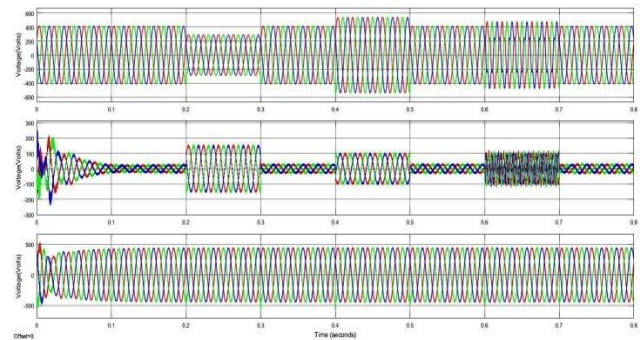
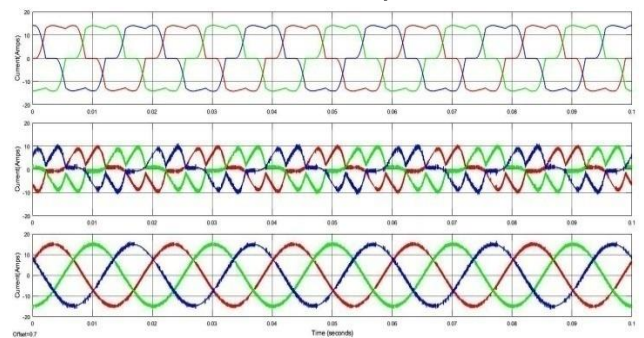


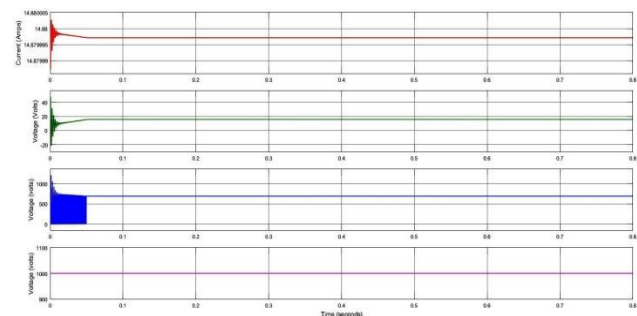
Fig. 15. PF for test cases



(a) V_s, V_{inj}, V_l

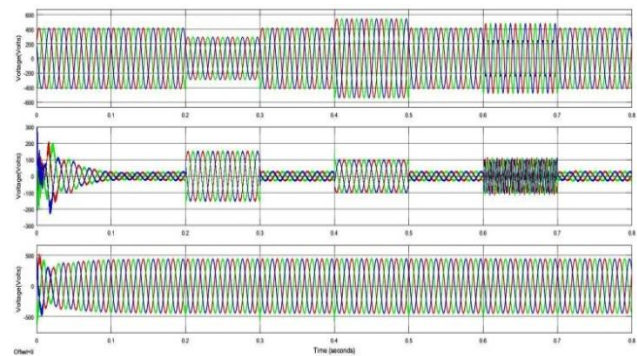


(b) i_l, i_{inj}, i_s

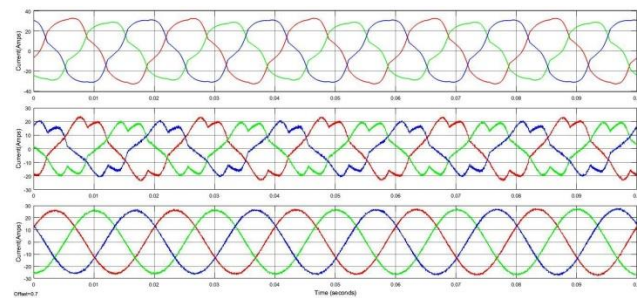


(c) I_{PV} , V_{PV} , V_{dc} , G

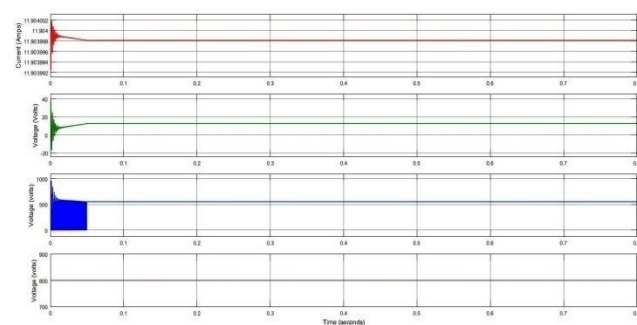
Fig. 16. Waveforms of proposed system for case-1



(a) V_S , V_{inj} , V_l

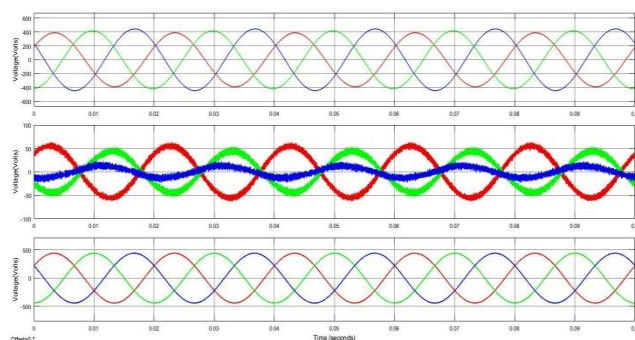


(b) i_l , i_{inj} , i_S

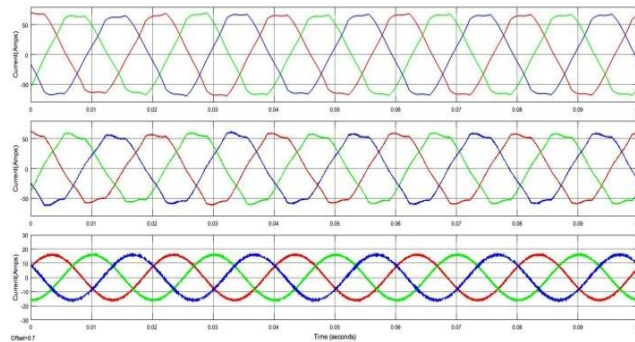


(c) I_{PV} , V_{PV} , V_{dc} , G

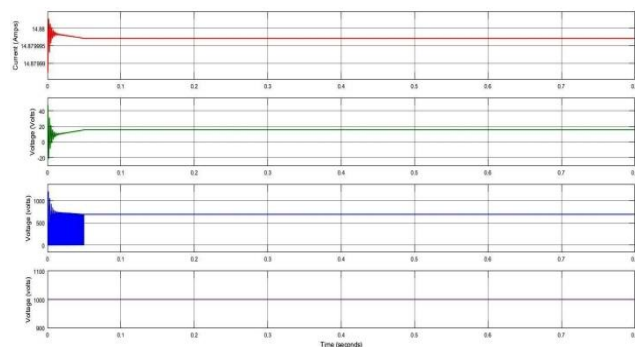
Fig. 17. Waveforms of Proposed system for case-2



(a) V_S , V_{inj} , V_l

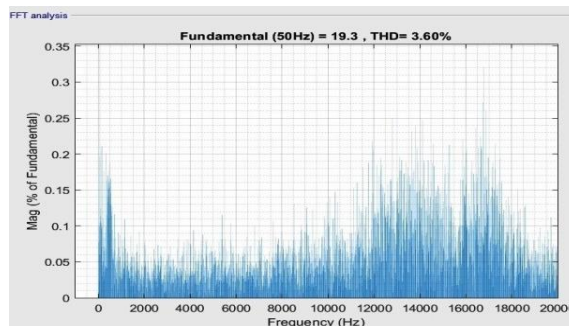


(b) I_l , I_{inj} , I_S



(c) I_{PV} , V_{PV} , V_{dc} , G

Fig. 18. Waveforms of Proposed system for case-3



Case 1

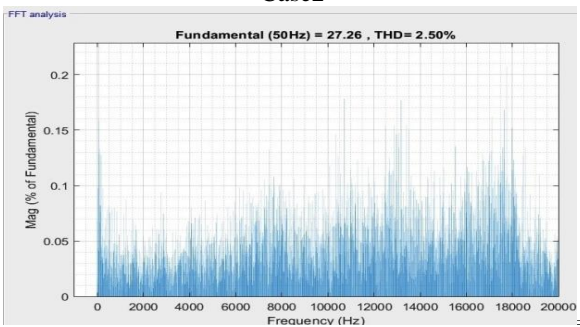
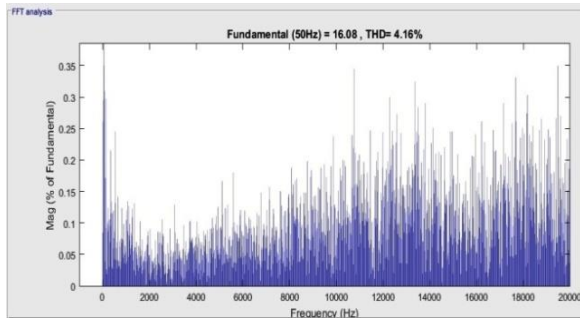


Fig. 19. THD spectrum for case studies

3. Conclusion

A hybrid controller involving FL-C and ANN controller was proposed for U-PVB. The design of BS and SP were given in addition to developing NFHC for shunt SVC controllers with a goal of achieving fast action in balancing dc-link voltage, eliminating sags/swells in supply voltage, minimizing the THD in load voltage and source current, and improving the power factor under balanced and unbalanced supply voltage conditions. The study on three test cases with different load combinations, balanced and unbalanced source voltages, voltage sag and swells, and variation on irradiation with constant temperature clearly exhibited that the NFHC was able to improve power factors almost unity. Moreover, the performance in minimizing THD to 3.6%, 4.16%, and 2.5% for all the three test cases were 15% better than those of the existing controllers. In addition, the NFHC took a smaller time to reach the steady-state DC-link voltage which is 50% less when compared to PI-C, SM-C, FL-C. The proposed model can further be studied on distribution systems with the micro-grid as future work. Moreover, the hybrid controller concept can be extended for the series VSC of UPQC.

References

1. Y. Wang, and M. Wong, "Historical Review of Parallel Hybrid Active Power Filter for Power Quality Improvement", IEEE TENCON, Jan 2015.
2. M. Kesler and E. Ozdemir, "Synchronous-Reference-Frame-Based Control Method for UPQC under Unbalanced and Distorted Load Conditions", IEEE Transactions on Industrial Electronics, Vol. 58, No. 9, pp. 3967-3975, September 2011.

3. M. Suresh and A. K. Panda, "PI and Fuzzy Logic Controller based 3-phase 4-wire Shunt active filter for mitigation of Current harmonics with Id-Iq Control Strategy", Journal Of Power Electronics, Springer, Vol. 11, No. 6, Nov 2011.
4. P. Kirawanich, and M.O.C. Robert, "Fuzzy Logic Control of an Active Power Line Conditioner", IEEE Transactions on Power Electronics, Vol. 19, No.6, Nov 2004.
5. M. Suresh and A. K. Panda, "RTDS hardware implementation and simulation of SHAF for mitigation of harmonics using p-q control strategy with PI and Fuzzy logic controllers", Frontiers of Electrical and Electronic Engineering , Springer, Vol. 7, No. 4, pp. 427-437, June 2012.
6. C.L. Hsiung, "Intelligent Neural Network-Based Fast Power System Harmonic Detection," IEEE Transactions on Industrial Electronics, Vol. 54, No. 1, pp. 43-52, Feb 2007.
7. S. Devassy, BhimSingh, "Design and Performance Analysis of Three-Phase Solar PV Integrated UPQC", IEEE 6th International Conference on Power Systems, Oct 2016.
8. P. K. Dash S. K. Panda T. H. Lee, J. X. Xu, A. Rou tray, "Fuzzy and Neural Controllers for Dynamic Systems: an Overview". Proceedings of Second International Conference on Power Electronics and Drive Systems, pp. 810-816, May 1997.
9. G.B. Mohankumar and S. Manoharan, "Performance Analysis of Multi Converter Unified Power Quality Conditioner with Dual Feeder System using Fuzzy Logic Control", International Journal of Control and Automation, Vol. 8, No. 3, pp. 251-270. March 2015.
10. M. Almelian, I. Mohd, M. Omran and U. U.Sheikh, "Performance of unified power quality conditioner (UPQC) based on fuzzy controller for attenuating of voltage and current harmonics", IOP Conf. Series: Materials Science and Engineering, Vol.3, No.1, pp. 012-084, April 2018.
11. V. Vinothkumar, R. Kanimozhi, "Power flow control and power quality analysis in power distribution system using UPQC based cascaded multi-level inverter with predictive phase dispersion modulation method", Journal of Ambient Intelligence and Humanized Computing, Springer, Vol.12, pp. 6445-6463, 2021.
12. M. R. Mohanraj, R. Prakash, "A Unified Power Quality Conditioner for Power Quality Improvement in Distributed Generation Network Using Adaptive Distributed Power Balanced Control (ADPBC)", International Journal of Wavelets, Multi-resolution and Information Processing, Vol. 18, No. 01, pp. 1941021, 2020.
13. K. Sarker, D. Chatterjee & S. K. Goswami, "A modified PV-wind-PEMFCS-based hybrid UPQC system with combined DVR/STATCOM operation by harmonic compensation", International Journal of Modeling and Simulation, World Scientific, Vol.41, No.4, pp. 243-255, March 2020.
14. S. S. Tejinder, S. Lakhwinder, B. Gill & M. Om Parkash, "Effectiveness of UPQC in Mitigating Harmonics Generated by an Induction Furnace",

- Electrical Power Components and Systems, Taylor & Francis, Vol. 46, No. 6, pp. 629-636, Nov-2018.
15. S.S. Dheeban & N.B. Muthu Selvan, "ANFIS-based Power Quality Improvement by Photovoltaic Integrated UPQC at Distribution System", IETE Journal of Research, Taylor & Francis, Feb-2021.
 16. H. Fujita, H. Akagi, "The unified power quality conditioner: The integration of series and shunt-active filters", IEEE Trans. Power Electronics, Vol. 13, No. 2, pp. 315-322, March 1998.
 17. V. Khadkikar, A. Chandra, "A new control philosophy for a unified power quality conditioner (UPQC) to coordinate load-reactive power demand between shunt and series inverters", IEEE Transactions on Power Delivery, Vol. 23, No. 4, pp: 2522-2534, Oct 2008.
 18. V.G. Kinhal, P. Agarwal, H.O. Gupta, "Performance investigation of neural-network-based unified power-quality conditioner", IEEE Transactions on Power Delivery, Vol. 26, No. 1, pp: 431-437, Jan 2011.
 19. V. Khadkikar, "Enhancing Electric Power Quality Using UPQC: A comprehensive Overview", IEEE Transactions on Power Electronics, Vol. 27, No. 5, pp. 2284 - 2297, May 2012.
 20. S. Samal and P. K. Hota, "Design and analysis of solar PV-fuel cell and wind energy based microgrid system for power quality improvement", Cogent Engineering, Taylor & Francis, Vol. 4, No. 1, pp. 1-22, Nov-2017.
 21. E. Nandhini and A. Sivaprakasam, "A Review of Various Control Strategies Based on Space Vector Pulse Width Modulation for the Voltage Source Inverter", IETE Journal of Research, Taylor & Francis, May-2020.
 22. F. Ayadi; I. Colak; I. Garip, H. Bulbul, "Impacts of Renewable Energy Resources in Smart Grid", 8th International Conference on Smart Grid, Paris, pp. 183-188, June 2020.
 23. I. Colak; R. Bayindir, S. Sagiroglu, "The Effects of the Smart Grid System on the National Grids", 8th International Conference on Smart Grid, Paris, pp. 122-126, June 2020.
 24. S. Jaber, A. M. Shakir, "Design and Simulation of a Boost-Microinverter for Optimized Photovoltaic System Performance", International Journal of Smart Grid, Vol. 5, No. 2, pp. 1-9, June 2021.
 25. S. Ikeda, F. Kurokawa, "Isolated and wide input ranged boost full bridge DC-DC converter for improved resilience of renewable energy systems", San Diego, CA, USA, pp. 290-295, 5-8 Nov. 2017.
 26. S. S. Dash, "Tutorial 1: Opportunities and challenges of integrating renewable energy sources in smart" 6th International Conference on Renewable Energy Research and Applications, San Diego, CA, USA, 5-8 Nov. 2017.
 27. M. Tsai, C. Chu, W. Chen, "Implementation of a Serial AC/DC Converter with Modular Control Technology", 7th International Conference on Renewable Energy Research and Applications, Paris, France, pp. 245-250, Oct. 2018.
 28. A. Thakallapelli, S. Ghosh; S. Kamalasan, "Real-time frequency based reduced order modeling of large power grid" IEEE Power and Energy Society General Meeting Boston, MA, USA, 17-21 July 2016.
 29. A. Belkaid, I. Colak, K. Kayisli, R. Bayindir, Improving PV System Performance Using High Efficiency Fuzzy Logic Control, 8th International Conference on Smart Grid, Paris, pp.152-156, June 2020.